Research Article Vol. 4, No. 9 / September 2017 / Optica 1059

Injection locking of a terahertz quantum cascade laser to a telecommunications wavelength frequency comb

Joshua R. Freeman,[1,*] Lalitha Ponnampalam,[2] Haymen Shams,[2] Reshma A. Mohandas,[1] Cyril C. Renaud,[2] Paul Dean,[1] Lianhe Li,[1] A. Giles Davies,[1] Alwyn J. Seeds,[2] and Edmund H. Linfield[1]

[1]Institute of Microwaves & Photonics, University of Leeds, Leeds LS2 9JT, UK
[2]Department of Electronic and Electrical Engineering, University College London, London WC1E 7JE, UK
*Corresponding author: j.r.freeman@leeds.ac.uk

Received 28 April 2017; revised 13 July 2017; accepted 26 July 2017 (Doc. ID 294781); published 1 September 2017

High-resolution spectroscopy not only can identify atoms and molecules but also can provide detailed information on their chemical and physical environment and relative motion. In the terahertz frequency region of the electromagnetic spectrum, where many molecules have fundamental vibrational modes, there is a lack of powerful sources with narrow linewidths that can be used for absorption measurements or as local oscillators in heterodyne detectors. The most promising solid-state source is the THz frequency quantum cascade laser (QCL), however, the linewidth of this compact semiconductor laser is typically too broad for many applications, and its frequency is not directly referenced to primary frequency standards. In this work, we injection lock a QCL operating at 2 THz to a compact fiber-based telecommunications wavelength frequency comb, where the comb line spacing is referenced to a microwave frequency reference. This results in the QCL frequency locking to an integer harmonic of the microwave reference, and the QCL linewidth reducing to the multiplied linewidth of the microwave reference, <100 Hz. Furthermore, we perform phase-resolved detection of the locked QCL and measure the phase noise of the locked system to be −75 dBc/Hz at 10 kHz offset from the 2 THz carrier.

OCIS codes: (140.3520) Lasers, injection-locked; (140.5965) Semiconductor lasers, quantum cascade; (040.2235) Far infrared or terahertz; (120.5050) Phase measurement.
https://doi.org/10.1364/OPTICA.4.001059

1. INTRODUCTION

The locking of one oscillator to another when there is a degree of coupling between them is a universal phenomenon that was first observed by Huygens in 1665 and later described by Adler [1]; it applies equally well to mechanical, electronic, and optical oscillators. For most applications, a weaker "master" oscillator with desirable temporal and spectral characteristics is used to control the output of a more powerful "slave" oscillator by coupling, or "injecting," the "master" oscillation into the "slave" oscillator. This technique has become ubiquitous in many areas of science and technology, and particularly in (ultra-)high-resolution spectroscopy and for the distribution of frequency standards.

High-resolution spectroscopy is a fundamental technique that finds application across a wide range of science and technology. It can be used to identify atoms and molecules through spectral fingerprinting; provide richly detailed information on the immediate chemical and physical environment, and relative motion, of the chemical species; and test fundamental theories of matter. Although high-resolution spectroscopy is well established in the visible and near-infrared (near-IR) regions of the spectrum, such application in the far-IR or terahertz (THz) region is poorly developed because of the lack of compact, stable, narrowband sources. To give one important example, astronomical spectroscopy commonly uses heterodyne detection to measure THz frequency emission from distant objects [2,3]. This passive technique uses a mixer and a local oscillator (LO) to measure weak signals close to the frequency of the narrow linewidth LO. Traditionally, LO THz sources based on gas lasers have been used, but these are bulky, confined to particular gas lines, and difficult to package in a form suitable for satellite-based instruments.

Another area of contemporary importance that requires high-resolution THz frequency sources is in the trapping and cooling of molecules [4,5]. Ultra-high-resolution spectroscopy of ultracold molecules in the THz spectral region would enable the investigation of fundamental physical constants [6,7], the particle physics standard model [8], and help determine molecular structure [9].

For these reasons, there has been significant interest in improving both the resolution and compactness of spectrometry in the THz spectral region. For frequencies below ~1.5 THz, frequency multiplier chains have been used both as LOs in heterodyne spectroscopy [10] and as narrowly tunable sources for transmission spectroscopy of cold molecules [11,12]. There has also been use of continuous-wave (CW) THz photomixers to provide emission at 0.6 THz and 1.2 THz, driven by a pair of diode lasers [13]; here the driving lasers were stabilized using a wavelength meter to achieve a THz emission linewidth of 4 MHz.

In the spectral region from 1.5 to 5 THz, however, the power available from frequency multiplier chains becomes impracticably small, and, as such, the most promising source is the THz quantum cascade laser (QCL) [14]. QCLs are electrically pumped semiconductor lasers operating across the mid-IR and THz spectral regions. They are compact, are high power [15], can be engineered to operate broadband or single mode, and can also show spontaneous frequency comb operation [16]. The linewidth of a QCL is intrinsically narrow [17] and exhibits a near-zero linewidth enhancement factor [18,19], but a free-running device has typically a much broader linewidth, around 1–2 MHz over short time scales [20] and up to 10 MHz over several seconds [21]. It therefore requires stabilization or locking for high-resolution applications.

To date, locking of THz QCLs to a gas line [22], a frequency multiplier chain [23,24], a femtosecond laser [20], and a femtosecond laser comb [25] has been demonstrated, and very recently, the locking of a mid-IR QCL to a frequency comb has been shown, with the latter derived from a traceable frequency standard and based on a nonlinear difference frequency generation technique [26]. However, all of these demonstrations made use of a negative feedback loop with a limited loop-bandwidth (a phase-locked loop) to provide a negative feedback voltage onto the QCL rather than the direct injection locking observed by Huygens. A direct injection approach has a simpler implementation, does not require a sensitive detector, overcomes the requirement for low loop delay, and can compensate for phase fluctuations over a wide bandwidth. Furthermore, the need to lock to a gas line or a femtosecond laser via a phase-locked loop results in a system that is either bulky, limited to particular frequencies, or both, which constrains its use for many potential applications.

In this work, we demonstrate injection locking of a QCL operating at a frequency around 2 THz to an all-fiber telecommunications-frequency comb, which has great potential for compact integration in photonic circuits. Locking is achieved by selecting a pair of comb lines from the near-IR comb and generating a difference frequency injection locking signal from them, close to the frequency of the free-running QCL. This THz difference frequency is then coupled into the QCL to injection lock it.

2. RESULTS

Our near-IR comb source uses a narrow linewidth C-band laser to seed an amplified fiber loop incorporating a high-speed phase modulator, driven by a microwave frequency synthesizer that determines the comb line spacing (see Supplement 1) [27]. The fiber loop operates as a resonant cavity and multiplies the number of comb lines produced by the phase modulator. The resulting all-fiber frequency comb generates over 125 lines and spans >2.7 THz, centered around 1552.5 nm. The comb line spacing is exactly equal to the microwave modulation frequency, f_{RF}, which can be adjusted in discrete steps from 18.5 to 20 GHz (see Supplement 1 for further details). It is important to note that while the linewidth of each comb line is determined by the linewidth of the seed laser (here 15 kHz), for this work, we use the heterodyne between two selected comb lines. For an ideal system, the linewidth of this heterodyne signal is N times the linewidth of the microwave reference (<1 Hz), where N is the number of comb lines separating the two selected lines.

The experimental arrangement used for injection locking the THz QCL is shown in Fig. 1. The microwave frequency synthesizer is set to $f_{RF} = 19.773076000$ GHz to control the spacing of the near-IR comb. The comb signal is split and filtered to obtain two comb lines that are separated by a frequency f_{THz} close to the THz QCL frequency (~1.97 THz). For $N = 101$, we find $f_{THz} = 1997.080676$ GHz($f_{THz} = 101 \times f_{RF}$), and this is the THz reference frequency to which the QCL is locked. The two comb lines required are selected by a wavelength selective switch, and each selected line is used to injection lock a separate tunable telecommunications wavelength laser (DS-DBR laser from Oclaro Technologies, UK). The signals from these lasers are then combined, amplified by an erbium-doped fiber amplifier (EDFA), and split by a 50:50 optical power splitter, with one portion sent to a fiber-coupled CW THz transmitter (Tx) and the second portion sent to a fiber-coupled CW THz receiver (Rx) (both supplied by Toptica Photonics; further details are in Supplement 1). A variable delay can be introduced into the receiver arm to control the relative phase between the THz signal arriving at the receiver from the QCL and the near-IR signal beating at THz reference frequency. The current induced in the receiver can be expressed as

$$I_{Rx} \propto G_p(\omega, t) E_{QCL}(\omega, t),$$

where G_p is the time varying conductance of the receiver active area due to the pair of locked diode lasers beating at the THz reference frequency, f_{THz}, and E_{QCL} is the THz field arriving at the antenna, oscillating at the THz QCL frequency, f_{QCL}. The full expression is given in Supplement 1. The current I_{Rx} is amplified by a transimpedance amplifier and captured on an oscilloscope. The intrinsic low-pass filtering of the receiver and

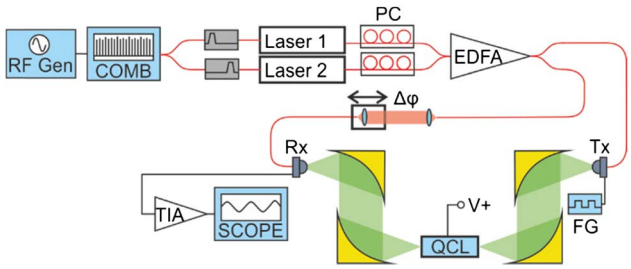

Fig. 1. Experimental arrangement used for injection locking the THz QCL. Electronic connections are shown in black, fiber connections and near-IR are in red, and free-space THz radiation is in green. Also shown, from the top left, are the RF signal generator (RF Gen); the wideband comb source (COMB); tunable bandpass filters; tunable DBR lasers, laser 1 and laser 2; polarization controllers (PC); an erbium-doped fiber amplifier (EDFA); the continuous-wave THz transmitter (Tx); a function generator (FG); the quantum cascade laser (QCL); a free-space optical delay line for phase adjustment ($\Delta\psi$); the continuous-wave THz receiver (Rx); a transimpedance amplifier (TIA); and an oscilloscope (SCOPE) for data acquisition.

amplifier results in a detected signal oscillating at the difference frequency of the THz reference and the QCL, $|f_{THz} - f_{QCL}|$. Photomixing receivers of this type [28] are typically used as homodyne detectors where the detected THz signal is derived from the same pair of lasers as the reference frequency. This produces a DC current that is proportional to the electric field of the THz radiation incident on the detector. However, these receivers are intrinsically fast (typical response times of 0.5 ps) [29,30] and therefore also function well as a frequency mixer. The beat frequency detection bandwidth is limited by the need to amplify the small current, and the trade-off between gain and bandwidth in the amplifier. For this work, a transimpedance amplifier provided a variable gain of 10^5, 10^6, or 10^7 Ω, corresponding to detection −3 dB bandwidths of 14 MHz, 1.8 MHz, and 50 kHz, respectively.

The QCL chosen for this work was a bound-to-continuum design that operates around 1.97 THz [31]. The QCL was fabricated with a single plasmon waveguide [32] and mounted on the cold finger of a continuous-flow helium cryostat, which was maintained at a temperature of 14 K. The electrical and optical characteristics of the device are shown in Fig. 2. To tune the frequency of the QCL to be close to f_{THz}, the operating current was chosen to be close to 775 mA, where the emission, measured by a high-resolution Fourier transform infrared spectrometer (FTIR), was single mode at 1.997 THz, marked by a blue dashed line in the figure. Further details on the QCL device are given in Supplement 1.

After basic characterization, the QCL device was mounted in the experimental arrangement shown in Fig. 1 and carefully aligned to maximize coupling of the CW THz radiation from the transmitter into the QCL cavity. To reduce heating in the transmitter, its bias was pulsed at a frequency of 1.15 kHz, with 50% duty cycle. This also allowed monitoring of the locked and unlocked signals in real time and also provided a reference signal for lock-in detection.

The measured heterodyne beat frequency between the QCL and the THz reference frequency, captured over 10 ms, is shown in Fig. 3 as a function of QCL drive current and, hence, frequency. The heterodyne signal with the THz transmitter turned off is shown in black; the QCL current is tuned to adjust the beat

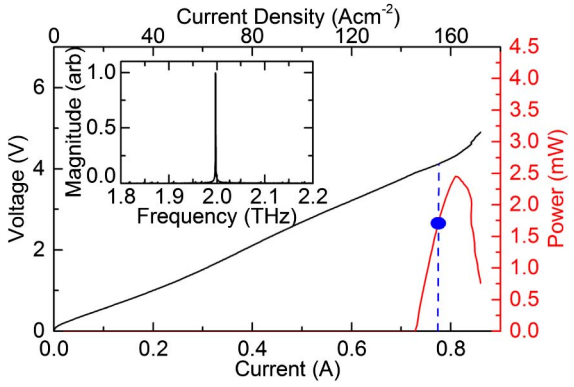

Fig. 2. I–V characteristics and THz output of the QCL. The device is operated in continuous wave with a heat sink temperature of 14 K. The blue dot marks the operating current used in this work (775 mA). The spectrum acquired at this operating point, when the QCL is free-running, is shown in the inset. The resolution for this spectrum is 250 MHz and shows a single lasing mode.

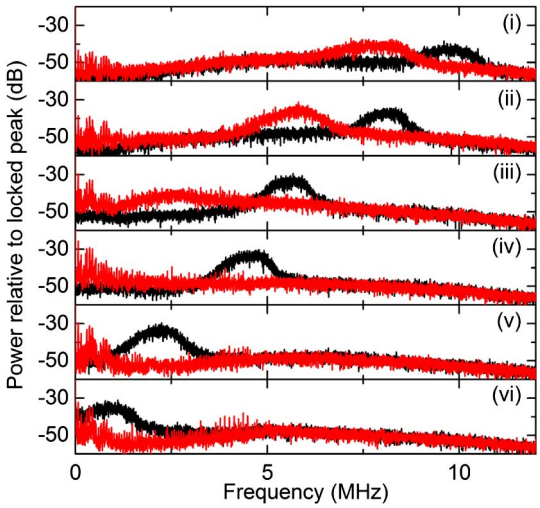

Fig. 3. Beat signal between the reference signal derived from the comb source and the QCL for the THz transmitter is off (black) and on (red). The QCL current is adjusted to tune the QCL frequency. The QCL current is adjusted over a range of 1.5 mA to tune the QCL emission frequency over the 9 MHz range shown in the figure.

frequency, with a measured tuning sensitivity of 6.5 MHz/mA. The FWHM (3 dB width) of the beat signal is measured to be 1.0 MHz with a 10 dB width of around 1.8 MHz, thought to be limited by noise in the QCL current source (Keithley 2400). The effective linewidth of the reference signal was calculated from the measured linewidth of the microwave frequency synthesizer (<1 Hz, limited by the resolution of the measurement) to be <100 Hz; therefore, the observed broadening of heterodyne signal can be assumed to arise entirely from the free-running QCL. This is in good agreement with previous measurements of free-running THz QCL linewidths [20], which are much larger than the quantum-limited intrinsic linewidths that THz QCLs of this type have shown [17]. Over longer time scales (∼minutes), there is a larger drift in QCL frequency caused by thermal fluctuations and mechanical vibrations; these could be reduced by using a bath cryostat rather than the continuous-flow cryostat that we used here.

The same axes also show the equivalent spectra when the transmitter is switched on (red). Upon switching the THz transmitter on, a significant amount of frequency pulling is observed immediately, with a frequency jump of ∼2 MHz for a frequency difference between the free-running QCL and reference frequency of 10 MHz [Fig 3(a), panel (i)]. As the heterodyne frequency between the QCL and THz reference frequency is reduced by tuning the QCL current, this frequency pulling effect increases until, for frequency differences less than ∼5 MHz [Fig. 3(a), panels (iv)–(vi)], the heterodyne beat is no longer visible when the transmitter is switched on. At this point, all of the signal appears at zero frequency (DC), and the QCL is injection locked to the reference frequency. The vertical axis of Fig. 3 shows relative power, in dB, to the peak signal at zero frequency when the QCL is locked. The QCL typically remains injection locked for up to few minutes before the lock is lost, thought to be caused by thermal fluctuations outside the locking range.

To obtain an indication of the QCL locking range, $\Delta\nu_{lock}$, we plot the ratio of the integrated noise (0–10 MHz) obtained with the transmitter on and off, as a function of heterodyne peak

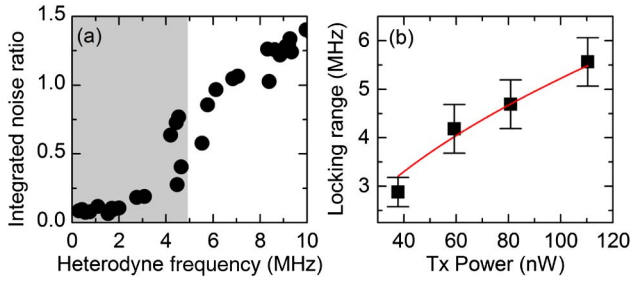

Fig. 4. (a) Integrated noise (0–10 MHz) as a function of the heterodyne beat signal position. The shaded region indicates the heterodyne frequencies for where the QCL becomes locked. (b) The observed locking range as a function of Tx power, showing a least-squares fitting to Adler's equation.

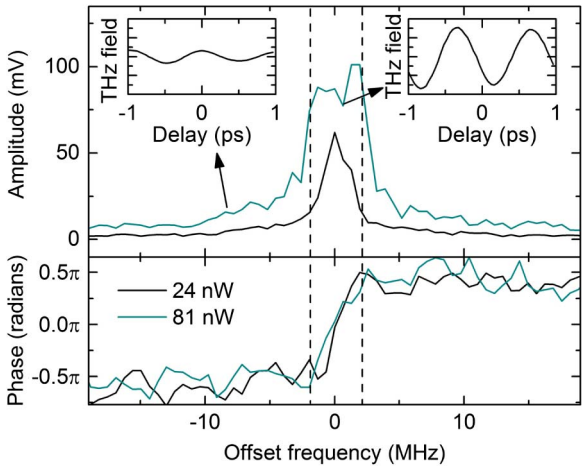

Fig. 5. Amplitude and phase of the locked signal measured using a lock-in amplifier. The frequency of the QCL is adjusted via its drive current and converted to frequency using the measured dependence of –6.5 MHz/mA. For each current (frequency) value, the detection phase is scanned and the sinusoidal waveform from the receiver recorded on the lock-in amplifier (shown in the insets). The amplitude and phase of this signal are shown for two injection powers. Because the detection is coherent, only QCL signals phase-locked to the comb will lead to a measurable signal.

position for the free-running QCL, Fig. 4(a). The figure shows a marked reduction in noise when the peak of the heterodyne signal is less than 5 MHz, which implies a full width locking range of 10 MHz. Figure 4(b) shows the locking range observed from the QCL for different Tx powers, P_{Tx}. The fit confirms that the expected relationship is observed, $\Delta\upsilon_{\mathrm{lock}} \propto \sqrt{P_{\mathrm{Tx}}}$.

We can compare the measured locking range of the THz QCL to the expected locking range using the simple expression derived by Adler [1]:

$$\Delta\upsilon_{\mathrm{lock}} \approx \frac{2\upsilon_0}{Q_e}\sqrt{\frac{P_1}{P_0}},$$

where ν_0 is the frequency of the oscillator, Q_e is the cavity quality factor, P_1 is the injected power, and P_0 is the free-running oscillator power. The Q-factor of the QCL is calculated to be $Q_e = 312$ (details are in Supplement 1). The power measured from the QCL at the operating current (775 mA) is $P_0 = 1.7$ mW, while the power measured from the transmitter is 100 nW for the data shown in Fig. 3. To obtain an estimate of P_1, the power coupled into the QCL cavity, we must take account of the coupling efficiency between the transmitter and the QCL, which, by calculating the overlap between the QCL mode and the focused transmitter beam, and the cryostat window losses, we estimate to be 8%. This leads to an estimated locking range of 28 MHz, larger than the measured value of 10 MHz; we attribute this difference to imperfect alignment between the transmitter and QCL. The above equation and the value of the calculated Q-factor for the QCL highlight the fact that THz QCLs are well suited to injection locking because of the low Q-factors these lasers typically possess. Furthermore, the locking range could be increased by improving the coupling between the transmitter and the QCL, for example, by integrating the transmitter with the QCL and avoiding free-space transmission. For a laser with a non-zero linewidth enhancement factor, the locking range becomes asymmetric about ν_0, and indeed, this effect has been used to measure the linewidth enhancement factor [33], but this is expected to be small in QCLs [18].

In addition to measuring the heterodyne beat for the locked and free-running QCL, we can make use of the control that is available over the phase of the reference signal to measure both the amplitude and phase of the locked QCL signal (Fig. 5). For this measurement, the length of the optical path to the THz receiver is varied using a free-space optical delay line (labeled $\Delta\psi$ in Fig. 1). This changes the relative phase of the reference signal with respect to the QCL signal, and by recording this sinusoidal signal for different QCL tunings, the amplitude and phase of the locked QCL signal can be measured. For these measurements, the gain of the transimpedance amplifier was increased to 10^6 Ω (bandwidth 1.8 MHz), and the signal was measured using a lock-in amplifier. The lock-in amplifier, together with the reduced transimpedance amplifier bandwidth, ensures that only QCL signals that are locked can be measured. The results are plotted in Fig. 5 for two different injection powers: when the QCL is well locked ($P_{\mathrm{Tx}} = 81$ nW) and when only partially locked ($P_{\mathrm{Tx}} = 24$ nW). The QCL is partially locked when the locking range is roughly equal to the linewidth such that it is locked and unlocked rapidly. The locked signal amplitude increases as the frequency of the QCL approaches the edge of the locking range. When in the locked range, the amplitude of the signal is flat, within the noise level, but the phase of the signal changes from $-\pi/2$ to $+\pi/2$, as expected from the analysis of Adler [1]. The amplitude of the locked signal (~90 mV) agrees with expected value given that the amplitude for the signal from the transmitter is 0.65 mV in this case, giving a power ratio of ~19, 000, close to the expected $P_{\mathrm{QCL}}/P_{\mathrm{Tx}} \sim 21,000$. When the injection power is reduced so that the QCL is never fully locked, the phase change is still observed, but the amplitude does not reach a plateau. The reduced locking range observed in Fig. 5 compared with Fig. 3 is due to the non-optimized alignment of the transmitter with the QCL in the data shown in Fig. 5.

The oscillator noise of the locked QCL shown in Fig. 6 is calculated from the receiver signal when the QCL is locked. For this, the detection bandwidth is increased to 14 MHz here, so both coherent (locked) signals and incoherent (unlocked) signals are measured. Since the noise is calculated from the measured spectrum, it includes components of both amplitude and phase noise. The measured noise when the heterodyne signal lies outside the

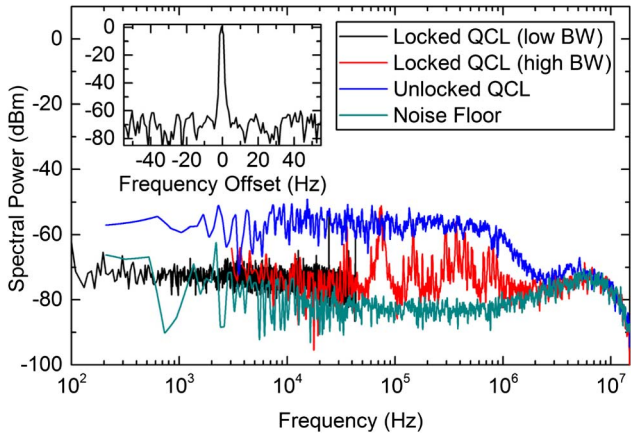

Fig. 6. Measured noise for the locked and unlocked QCL. For the locked QCL, two traces are shown, acquired using two different gain (bandwidth) settings for the transimpedance amplifier to cover both low and high frequencies. The noise floor is also indicated, measured by tuning the QCL frequency away from the reference frequency so that the heterodyne beat lies outside the detection bandwidth. The inset shows the heterodyne beat between the locked QCL and the THz reference frequency.

detection bandwidth (>20 MHz) is also shown, to indicate the noise floor of the measurement system, together with the corresponding noise for the unlocked QCL. Apart from a peak at 75 kHz (which is thought to be from the delay stage motion controller) and some further peaks in the 100 kHz–1 MHz range, the phase noise of the locked QCL follows the noise floor of the measurement system over the five decades of frequency shown.

Finally, to indicate the linewidth achievable from the QCL, we present the heterodyne beat signal between the THz reference frequency derived from the optical comb and the locked QCL in the inset to Fig. 6. The 10 dB linewidth of the beat signal is ∼2 Hz, limited by the resolution of the measurement, implying a sub-Hz FWHM. However, if a Lorentzian lineshape is assumed, and the FWHM is calculated from the phase noise at 100 Hz offset (∼ − 70 dBc/Hz), then a value 1 order of magnitude below this (<100 mHz) is found. While the absolute linewidth of the locked QCL cannot be reduced below that of the THz reference signal (measured to be <100 Hz in the present case), this indicates the locked QCL linewidths that ought to be achievable with a lower phase noise microwave reference source.

3. CONCLUSION

In conclusion, we have injection locked a THz QCL operating at 2 THz to a near-IR fiber-based optical frequency comb. This not only stabilizes the frequency of the QCL so it becomes traceable to the microwave reference frequency but also allows the phase-locked CW QCL emission to be detected coherently. This brings the same high levels of frequency precision and accuracy that are available in the microwave region to the THz region of the spectrum.

While in this work the comb spacing (and therefore the THz reference frequency) is only tunable in discrete steps, continuous tunability could be implemented with the use of an optical phase-locked loop [34] replacing one of the locked DBR lasers. This would allow continuous tuning of the locked QCL across its full gain-bandwidth. By implementing a slow-feedback to the QCL bias, forming an optical injection phase-locked loop [35], the QCL could be made to track the reference frequency across a large bandwidth. This would also improve long-term stability.

For applications, this scheme is very appealing, particularly since very compact integration should be possible given that all components are semiconductor based; the fiber loop and tunable telecommunications wavelength lasers can be monolithically integrated on-chip as photonic integrated circuits [36]. Furthermore, the QCL and photomixer could be integrated, eliminating the free-space path, making use of only a fiber connection and so reducing the need for alignment.

The work described here enables referencing of THz sources to primary frequency standards in an experimentally convenient format. To use this template, you will need to apply the embedded styles to each paragraph-level item in your manuscript or simply use this template as a visual guide.

The data associated with this paper are openly available from the University of Leeds data repository [37].

Funding. Engineering and Physical Sciences Research Council (EPSRC) (EP/J002356/1, EP/J017671/1); Seventh Framework Programme (FP7) (247375); Royal Society; Wolfson Foundation.

Acknowledgment. Support from the Royal Society and Wolfson Foundation (A. G. D. and E. H. L.) is acknowledged.

See Supplement 1 for supporting content.

REFERENCES

1. A. E. Siegman, *Lasers* (University Science Books, 1989).
2. S. Leurini, F. Wyrowski, H. Wiesemeyer, A. Gusdorf, R. Güsten, K. M. Menten, M. Gerin, F. Levrier, H. W. Hübers, K. Jacobs, O. Ricken, and H. Richter, "Spectroscopically resolved far-IR observations of the massive star-forming region G5.89-0.39," Astron. Astrophys. **584**, A70 (2015).
3. L. Rezac, P. Hartogh, R. Güsten, H. Wiesemeyer, H.-W. Hbers, C. Jarchow, H. Richter, B. Klein, and N. Honingh, "First detection of the 63 μm atomic oxygen line in the thermosphere of Mars with GREAT/SOFIA⋆," Astron. Astrophys. **580**, L10 (2015).
4. J. F. Barry, D. J. McCarron, E. B. Norrgard, M. H. Steinecker, and D. DeMille, "Magneto-optical trapping of a diatomic molecule," Nature **512**, 286–289 (2014).
5. E. B. Norrgard, D. J. McCarron, M. H. Steinecker, M. R. Tarbutt, and D. DeMille, "Submillikelvin dipolar molecules in a radio-frequency magneto-optical trap," Phys. Rev. Lett. **116**, 063004 (2016).
6. E. R. Hudson, H. J. Lewandowski, B. C. Sawyer, and J. Ye, "Cold molecule spectroscopy for constraining the evolution of the fine structure constant," Phys. Rev. Lett. **96**, 143004 (2006).
7. P. Jansen, H. L. Bethlem, and W. Ubachs, "Perspective: tipping the scales: search for drifting constants from molecular spectra," J. Chem. Phys. **140**, 010901 (2014).
8. J. Baron, W. C. Campbell, D. DeMille, J. M. Doyle, G. Gabrielse, Y. V. Gurevich, P. W. Hess, N. R. Hutzler, E. Kirilov, I. Kozyryev, B. R. O'Leary, C. D. Panda, M. F. Parsons, E. S. Petrik, B. Spaun, A. C. Vutha, and A. D. West, "Order of magnitude smaller limit on the electric dipole moment of the electron," Science **343**, 269–272 (2014).
9. O. Asvany, K. M. T. Yamada, S. Brünken, A. Potapov, and S. Schlemmer, "Experimental ground-state combination differences of CH5," Science **347**, 1346–1349 (2015).
10. H. W. Hubers, "Terahertz heterodyne receivers," IEEE J. Sel. Top. Quantum Electron. **14**, 378–391 (2008).
11. O. Asvany, O. Ricken, H. S. P. Müller, M. C. Wiedner, T. F. Giesen, and S. Schlemmer, "High-resolution rotational spectroscopy in a cold ion trap: H_2D^+ and D_2H^+," Phys. Rev. Lett. **100**, 233004 (2008).

12. J. Shen, A. Borodin, M. Hansen, and S. Schiller, "Observation of a rotational transition of trapped and sympathetically cooled molecular ions," Phys. Rev. A **85**, 032519 (2012).
13. S. Lee, D. Hauser, O. Lakhmanskaya, S. Spieler, E. S. Endres, K. Geistlinger, S. S. Kumar, and R. Wester, "Terahertz-visible two-photon rotational spectroscopy of cold OD^-," Phys. Rev. A **93**, 032513 (2016).
14. R. Köhler, A. Tredicucci, F. Beltram, H. E. Beere, E. H. Linfield, A. G. Davies, D. A. Ritchie, R. C. Iotti, and F. Rossi, "Terahertz semiconductor heterostructure laser," Nature **417**, 156–159 (2002).
15. L. Li, L. Chen, J. Zhu, J. Freeman, P. Dean, A. Valavanis, A. G. Davies, and E. H. Linfield, "Terahertz quantum cascade lasers with >1 W output powers," Electron. Lett. **50**, 309–311 (2014).
16. A. Hugi, G. Villares, S. Blaser, H. C. Liu, and J. Faist, "Mid-infrared frequency comb based on a quantum cascade laser," Nature **492**, 229–233 (2012).
17. M. S. Vitiello, L. Consolino, S. Bartalini, A. Taschin, A. Tredicucci, M. Inguscio, and P. De Natale, "Quantum-limited frequency fluctuations in a terahertz laser," Nat. Photonics **6**, 525–528 (2012).
18. R. P. Green, J.-H. Xu, L. Mahler, A. Tredicucci, F. Beltram, G. Giuliani, H. E. Beere, and D. A. Ritchie, "Linewidth enhancement factor of terahertz quantum cascade lasers," Appl. Phys. Lett. **92**, 071106 (2008).
19. Y. Leng Lim, P. Dean, M. Nikolić, R. Kliese, S. P. Khanna, M. Lachab, A. Valavanis, D. Indjin, Z. Ikonić, P. Harrison, E. H. Linfield, A. Giles Davies, S. J. Wilson, and A. D. Rakić, "Demonstration of a self-mixing displacement sensor based on terahertz quantum cascade lasers," Appl. Phys. Lett. **99**, 081108 (2011).
20. S. Barbieri, P. Gellie, G. Santarelli, L. Ding, W. Maineult, C. Sirtori, R. Colombelli, H. Beere, and D. Ritchie, "Phase-locking of a 2.7, THz quantum cascade laser to a mode-locked erbium-doped fibre laser," Nat. Photonics **4**, 636–640 (2010).
21. A. Barkan, F. K. Tittel, D. M. Mittleman, R. Dengler, P. H. Siegel, G. Scalari, L. Ajili, J. Faist, H. E. Beere, E. H. Linfield, A. G. Davies, and D. A. Ritchie, "Linewidth and tuning characteristics of terahertz quantum cascade lasers," Opt. Lett. **29**, 575–577 (2004).
22. H. Richter, S. G. Pavlov, A. D. Semenov, L. Mahler, A. Tredicucci, H. E. Beere, D. A. Ritchie, and H.-W. Hübers, "Submegahertz frequency stabilization of a terahertz quantum cascade laser to a molecular absorption line," Appl. Phys. Lett. **96**, 071112 (2010).
23. P. Khosropanah, A. Baryshev, W. Zhang, W. Jellema, J. N. Hovenier, J. R. Gao, T. M. Klapwijk, D. G. Paveliev, B. S. Williams, S. Kumar, Q. Hu, J. L. Reno, B. Klein, and J. L. Hesler, "Phase locking of a 2.7 THz quantum cascade laser to a microwave reference," Opt. Lett. **34**, 2958–2960 (2009).
24. D. Rabanus, U. U. Graf, M. Philipp, O. Ricken, J. Stutzki, B. Vowinkel, M. C. Wiedner, C. Walther, M. Fischer, and J. Faist, "Phase locking of a 1.5 terahertz quantum cascade laser and use as a local oscillator in a heterodyne HEB receiver," Opt. Express **17**, 1159–1168 (2009).
25. L. Consolino, A. Taschin, P. Bartolini, S. Bartalini, P. Cancio, A. Tredicucci, H. E. Beere, D. A. Ritchie, R. Torre, M. S. Vitiello, and P. De Natale, "Phase-locking to a free-space terahertz comb for metrological-grade terahertz lasers," Nat. Commun. **3**, 1040 (2012).
26. B. Argence, B. Chanteau, O. Lopez, D. Nicolodi, M. Abgrall, C. Chardonnet, C. Daussy, B. Darquié, Y. Le Coq, and A. Amy-Klein, "Quantum cascade laser frequency stabilization at the sub-Hz level," Nat. Photonics **9**, 456–460 (2015).
27. S. Bennett, B. Cai, E. Burr, O. Gough, and A. J. Seeds, "1.8-THz bandwidth, zero-frequency error, tunable optical comb generator for DWDM applications," IEEE Photon. Technol. Lett. **11**, 551–553 (1999).
28. K.-E. Peiponen, A. Zeitler, and M. Kuwata-Gonokami, *Terahertz Spectroscopy: Theory and Applications* (Springer, 2012).
29. S. Preu, G. H. Döhler, S. Malzer, L. J. Wang, and A. C. Gossard, "Tunable, continuous-wave terahertz photomixer sources and applications," J. Appl. Phys. **109**, 061301 (2011).
30. Y.-S. Lee, *Principles of Terahertz Science and Technology* (Springer, 2009).
31. J. R. Freeman, O. P. Marshall, H. E. Beere, and D. A. Ritchie, "Improved wall-plug efficiency of a 1.9 THz quantum cascade laser by an automated design approach," Appl. Phys. Lett. **93**, 191119 (2008).
32. B. S. Williams, "Terahertz quantum-cascade lasers," Nat. Photonics **1**, 517–525 (2007).
33. G. Liu, X. Jin, and S. L. Chuang, "Measurement of linewidth enhancement factor of semiconductor lasers using an injection-locking technique," IEEE Photon. Technol. Lett. **13**, 430–432 (2001).
34. K. Balakier, M. J. Fice, L. Ponnampalam, A. J. Seeds, and C. C. Renaud, "Monolithically integrated optical phase lock loop for microwave photonics," J. Lightwave Technol. **32**, 3893–3900 (2014).
35. C. Walton, A. C. Bordonalli, and A. J. Seeds, "High-performance heterodyne optical injection phase-lock loop using wide linewidth semiconductor lasers," IEEE Photon. Technol. Lett. **10**, 427–429 (1998).
36. C. C. Renaud, M. Pantouvaki, S. Gregoire, I. Lealman, P. Cannard, S. Cole, R. Moore, R. Gwilliam, and A. J. Seeds, "A monolithic MQW InP-InGaAsP-based optical comb generator," IEEE J. Quantum Electron. **43**, 998–1005 (2007).
37. "University of Leeds data repository," https://doi.org/10.5518/224.